Statistical crossover characterization of the heterotic localized-extended transition

Ryuichi Ugajin*

Fusion Domain Laboratory, Sony Corporation, 5-21-15 Higashikojiya, Ota-ku, Tokyo 144-0033, Japan

We investigated the spectral statistics of a quantum particle in a superlattice consisting of a disordered layer and a clean layer, possibly accompanied by random magnetic fields. Because a disordered layer has localized states and a clean layer has extended states, our quantum system shows a heterotic phase of an Anderson insulator and a normal metal. As the ratio of the volume of these two layers changes, the spectral statistics change from Poissonian to one of the Gaussian ensembles which characterize quantum chaos. A crossover distribution specified by two parameters is introduced to distinguish the transition from an integrable system to a quantum chaotic system during the heterotic phase from an Anderson transition in which the degree of random potentials is homogenous.

I. INTRODUCTION

It has been established that an integrable quantum system has energy levels whose nearest-neighbor spacing is well described by the Poisson distribution, where the energy-level sequence is purely random [1,2]. On the other hand, a quantum system whose classical counterpart is chaotic is characterized by one of the three Gaussian ensembles, namely, a Gaussian orthogonal ensemble (GOE), a Gaussian unitary ensemble (GUE), and a Gaussian symplectic ensemble (GSE), in which the energy-level sequence is affected by a strong repulsion between the energy levels [3–5]. These three ensembles are universal in the sense that information in a Hamiltonian is at a minimum, except that concerning its global symmetry [6]. The spectral statistics could be specified more precisely if one introduces more constraints on the Hamiltonian, e.g., a Hamiltonian being the sum of the deterministic and random parts [7] or a Hamiltonian having a particle-hole symmetry [8].

During the transition from integrable to quantum chaotic, there is a crossover region where the observed spectra can be attributed to neither Poissonian nor one of the universal Gaussian ensembles [9,10]. The Berry-Robnik distribution [11]

$$P_2(s,\rho) = \rho^2 e^{-\rho s} \, \text{erf}\left(\frac{\sqrt{\pi}\bar{\rho}s}{2}\right) + \left(2\rho\bar{\rho} + \frac{\pi\bar{\rho}^3 s}{2}\right) e^{-\rho s - \pi\bar{\rho}^2 s^2/4} \tag{1}$$

is one of the crossover distributions that have been used to characterize the nearest-neighbor spacing distribution of intermediate statistics between Poissonian and GOE, where $\bar{\rho} = 1 - \rho$ and

$$\text{erf}(x) = \frac{2}{\sqrt{\pi}} \int_x^\infty d\tau e^{-\tau^2} \tag{2}$$

is the error function. While $P_2(s,1)$ is identical to the Poisson distribution

$$P_P(s) = e^{-s}, \tag{3}$$

$P_2(s,0)$ is the same as predicted by GOE

$$P_{\text{GOE}}(s) = \frac{\pi s}{2} e^{-\pi s^2/4}. \tag{4}$$

The Berry-Robnik parameter ρ may be interpreted as the relative phase-space volume of the regular regions in the system's classical counterpart [12]. The Brody distribution [13]

$$P_B(s;\nu) = (\nu+1)a(\nu)s^\nu \exp[-a(\nu)s^{\nu+1}] \tag{5}$$

is also useful to characterize the observed spectrum using a single parameter ν, where $a(\nu)$ is a constant. The Brody parameter ν appears in the exponent of the factor s^ν, so it measures the strength of repulsion in the energy levels, i.e., $\nu=0$ for Poissonian and $\nu=1$ for GOE.

Let us consider a quantum system which depends on two parameters, i.e., V_1 and V_2. We assume that our system is integrable when $V_1 = V_2 = 0$ and shows quantum chaos when $V_1 = V_2 = 1$. We calculate the nearest-neighbor spacing distribution of our quantum system for each V_1 and V_2 to determine the Brody parameter as a function of V_1 and V_2, as in $\nu = f(V_1, V_2)$, where $f(0,0) = 0$ and $f(1,1) = 1$. It is obvious that we cannot catalog quantum systems using the inverse function of $f(V_1, V_2)$. There might be quantum systems with the same value of the Brody parameter, but their spectral statistics would be different. Note that the nearest-neighbor spacing distribution $P(s)$ is a probability distribution and is restricted only by $\int_0^\infty P(s)ds = 1$ and $\int_0^\infty sP(s)ds = 1$. Therefore, there are possibilities of intermediate distribution functions far beyond a distribution function determined by a single parameter. It would be interesting to know if there are quantum systems requiring intermediate statistics, where the nearest-neighbor spacing distribution must be described by more than a single parameter.

This paper considers a quantum particle in a superlattice structure of an *A* layer and a *B* layer, the first of which is an Anderson insulator and the second of which is a normal metal. While the *A* layer is full of impurities which generate

*Email address: Ryuichi.Ugajin@jp.sony.com

scattering centers, the B layer is relatively clean. Let us note that this system can be thought of as a heterosis of these two phases of electrons, i.e., an Anderson insulator and a normal metal, as in the heterosis of a ferromagnetic phase and paramagnetic phase [14]. It is expected that as the ratio of the volume of these two layers changes, the spectral statistics will undergo a transition from the Poissonian to the Gaussian ensemble. To distinguish this transition during the heterotic phase of an Anderson insulator and a normal metal from an Anderson transition when the degree of disorder is homogenous, we introduce a crossover characterization dependent on two parameters.

II. MODEL

Spectral statistics are known to be useful in determining the behavior of a quantum particle in a disordered medium [15–19]. This is because we know that the spectral statistics of an electron extended over random impurities are those of a quantum chaotic system which is characterized by strong repulsion between energy levels. On the other hand, the spectral statistics of localized electrons are Poissonian. In the phase of localized electrons, i.e., an Anderson insulator, if one assumes a state localized near a point, one should find another state localized near another point. If the localization length of the first state is similar to that of the second state, the energy difference between these two states is so small that there is no repulsion between these energy levels. As the degree of disorder increases, the spectral statistics change from those of a quantum chaotic system to a Poissonian, showing an Anderson transition [20–22]. When the Anderson transition occurs, the spectral statistics change from Poissonian to GOE if the electrons are affected by neither spin-orbit interactions nor magnetic fields [15]. During the transition from Poissonian to GOE, the spectral statistics may be well characterized by one of the crossover distributions noted previously. When a magnetic field breaks the time-reversal symmetry of the system, the quantum chaos will be characterized by GUE [23]. If spin-orbit interaction affects the level fluctuations, the strength of repulsion between energy levels would be as strong as predicted by GSE [24,25].

Let us introduce a cubic lattice of size L, whose sites are denoted by

$$\mathbf{r}_p = (x_p, y_p, z_p). \tag{6}$$

Operator $\hat{c}_p^\dagger$ creates a quantum particle at lattice site $\mathbf{r}_p$. A tight-binding Hamiltonian is written as

$$\hat{H} = -\sum_{\langle p,q \rangle} t_{p,q} \hat{c}_p^\dagger \hat{c}_q + \sum_p v_p \hat{c}_p^\dagger \hat{c}_p + \text{H.c.}, \tag{7}$$

where $\langle p,q \rangle$ is a pair of nearest-neighbor sites. Transfer $t_{p,q}$ is taken to be

$$t_{p,q} = \begin{cases} \exp(2\pi i\, \theta_{p,q}) & \text{when } |\mathbf{r}_p - \mathbf{r}_q| = 1 \\ 0 & \text{otherwise.} \end{cases} \tag{8}$$

We have introduced random variable $\theta_{p,q}$ which satisfies $\theta_{p,q} = -\theta_{q,p}$ and $|\theta_{p,q}| < \xi/2$. A random magnetic field can be introduced by $\xi > 0$. On-site random potential v_p is defined as

$$v_p = \begin{cases} -V_s/2 < v_p < V_s/2 & \text{when } 1 \leq z_p \leq M \\ -V_l/2 < v_p < V_l/2 & \text{when } M < z_p \leq L. \end{cases} \tag{9}$$

The periodic boundary condition is used for our lattice. Our quantum system is composed of two layers, one of which has thickness M and is disturbed by a random potential with the degree of V_s, and the other of which has thickness $L-M$ and is disturbed by a random potential with the degree of V_l. It is useful to investigate the case of $V_s = V_l$, which is an Anderson transition problem in which the degree of disorder is spatially homogenous. We now turn our attention to the case in which $V_s \neq V_l$, in particular, $V_s < V_c$ and $V_c < V_l$, where V_c is the critical degree of disorder of the Anderson transition. It is well known that V_c is about 16.5 in a three-dimensional cubic lattice [18].

We take $L = 24$, so the total number of sites is $L^3 = 13\,824$. $\hat{H}$ is numerically diagonalized, yielding eigenvalues ϵ_p ($p = 1, 2, \ldots, 13\,824$). We used 2000 levels from ϵ_{5913} to ϵ_{7912} in order to determine the spectral statistics. Before we determine the spectral statistics, however, the energy-level sequences must be modified by "unfolding" them using the third-order functions of energy, so as to give the energy-level sequences a constant density where the average of nearest-neighbor spacing is one [26]. The nearest-neighbor spacing distribution is evaluated as the probability $P(s)ds$ such that the energy difference between adjacent levels will be between s and $s + ds$. We take $ds = \frac{1}{10}$. The Δ_3 statistics of Dyson and Mehta are helpful in determining whether the off-diagonal elements of a Hamiltonian matrix constructed using the eigenfunctions of integrable systems strongly influence the behavior of the system. The Δ_3 statistics of Dyson and Metha are defined by the ensemble average of

$$\Delta(n) = \min_{A,B} \left(\frac{1}{2n} \int_{-n}^{n} [\lambda(\epsilon) - A\epsilon - B]^2 d\epsilon \right). \tag{10}$$

Therefore, we take the average of $\Delta(n)$ for many segments of energy levels in order to obtain $\Delta_3(n)$.

When $\xi > 0$ breaks the time-reversal symmetry, the quantum system whose classical counterpart is chaotic has the nearest-neighbor spacing distribution predicted by GUE:

$$P_{\text{GUE}}(s) = \frac{32 s^2}{\pi^2} e^{-4 s^2/\pi}, \tag{11}$$

which is compared to that of the GOE and the Poissonian distribution in Fig. 1. The crossover distribution specified by two parameters (ω, η) is given by

$$Q(s; \omega, \eta) = A(\omega, \eta) s^{2\omega} \exp[-B(\omega, \eta) s^{1+\eta}]. \tag{12}$$

The conditions

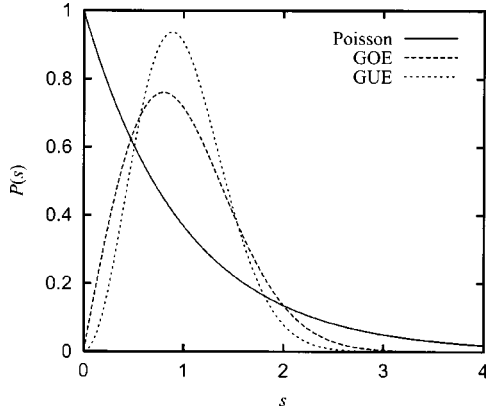FIG. 1. The nearest-neighbor spacing distribution $P(s)$ of GOE, GUE, and Poissonian.

$$\int_0^\infty ds\, Q(s;\omega,\eta) = 1 \qquad (13)$$

and

$$\int_0^\infty ds\, s\, Q(s;\omega,\eta) = 1 \qquad (14)$$

determine the coefficients $A(\omega,\eta)$ and $B(\omega,\eta)$ as

$$A(\omega,\eta) = (1+\eta)\frac{\left[\Gamma\left(\dfrac{2+2\omega}{1+\eta}\right)\right]^{1+2\omega}}{\left[\Gamma\left(\dfrac{1+2\omega}{1+\eta}\right)\right]^{2+2\omega}} \qquad (15)$$

and

$$B(\omega,\eta) = \left[\frac{\Gamma\left(\dfrac{2+2\omega}{1+\eta}\right)}{\Gamma\left(\dfrac{1+2\omega}{1+\eta}\right)}\right]^{1+\eta}, \qquad (16)$$

where

$$\Gamma(z) = \int_0^\infty dt\, t^{z-1} e^{-t} \qquad (17)$$

is the Gamma function. When the histogram of $P(s)$ obtained from the observed spectrum is denoted by $P^{(ex)}(s_j)$, we can determine the appropriate values of (ω,η) in order to minimize the deviation

$$\Theta(\omega,\eta) = \sum_{j=1}^{24} [Q(s_j;\omega,\eta) - P^{(ex)}(s_j)]^2. \qquad (18)$$

The two parameters (i.e., ω and η), have different roles in the crossover distribution. ω appears in the exponent of the factor $s^{2\omega}$ measuring the strength of repulsion between energy levels when they are close, i.e., when s is smaller than 1. η appears in the exponential function, measuring how fast the crossover distribution decays as s increases beyond 1.

When η is small, large intervals between adjacent levels are frequently seen in the energy spectrum. The Brody distribution is obtained when $\omega = \eta/2$. Because $Q(s;0,0)$ is Poissonian, i.e., $P_P(s)$, and $Q(s;1,1)$ is identical to $P_{GUE}(s)$, the route from $(\omega,\eta) = (0,0)$ to $(1,1)$ is accompanied by a transition from an integrable system to a quantum chaotic system characterized by GUE. Note that $Q(s;\frac{1}{2},1)$ is identical to the nearest-neighbor spacing distribution predicted by GOE and $Q(s;2,1)$ is that predicted by GSE.

III. SPECTRAL STATISTICS

A. Homogenous phase

When $V_s = V_l$, denoted by V, our system will show the spectral behavior of a system which exhibits an Anderson transition. This is because the degree of disorder is homogenous in the system. If V is sufficiently small, it shows a metallic behavior accompanied by quantum chaos. On the other hand, if V is sufficiently large, it possesses localized states whose energy levels are uncorrelated as in the Poisson distribution.

Figure 2 shows the nearest-neighbor spacing distribution $P(s)$ and the Δ_3 statistics of Dyson and Mehta when $V_s = V_l = V$ is changed from 10 to 40 with $\xi = 0$. In Fig. 2(a), $P(s)$ of the observed spectra is well approximated by the broken lines, i.e., the crossover distribution $Q(s;\omega,\eta)$ with appropriate values of (ω,η). In Fig. 2(b) we also show the Δ_3 statistics of the Poisson distribution,

$$\Delta_3(n) = \frac{n}{15}, \qquad (19)$$

and those predicted by GOE,

$$\Delta_3(n) = \frac{1}{\pi^2}\left[\ln(2\pi n) + \gamma - \frac{\pi^2}{8} - \frac{5}{4}\right] + O(n^{-1}), \quad (20)$$

where γ is Euler's constant [4]. When $V = 40$, the electronic structure is that of an integrable system consisting of localized states, so $P(s)$ is similar to the Poissonian distribution. On the other hand, when $V = 10$, the electronic structure is that of a quantum chaotic system consisting of extended states, so $P(s)$ is similar to that predicted by GOE. Figure 3 shows the nearest-neighbor spacing distribution $P(s)$ and the Δ_3 statistics of Dyson and Mehta when $V_s = V_l = V$ is changed from 10 to 40 with $\xi = 0.1$. In Fig. 3(a), the crossover distribution $Q(s;\omega,\eta)$ with appropriate values of (ω,η) are also shown. In Fig. 3(b), we also show the Δ_3 statistics predicted by GUE,

$$\Delta_3(n) = \frac{1}{2\pi^2}\left[\ln(2\pi n) + \gamma - \frac{5}{4}\right] + O(n^{-1}). \qquad (21)$$

Because of the existence of random magnetic fields, the time-reversal symmetry is broken, so the quantum chaos is characterized by GUE when the repulsion between energy levels is strong. Because the system is homogenous, this type
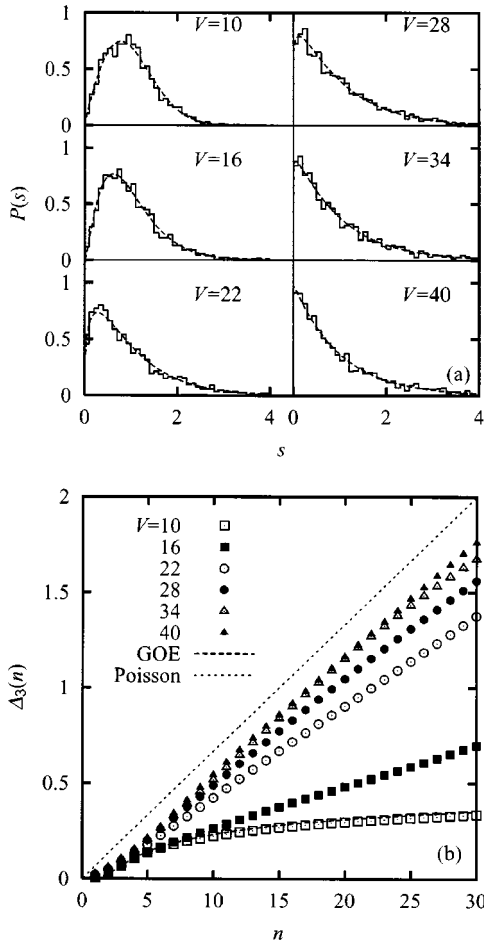
FIG. 2. The spectral statistics of a homogeneous phase without random magnetic fields $\xi = 0$ when V is taken to be 10, 16, 22, 28, 34, and 40. (a) The nearest-neighbor spacing distribution $P(s)$. The crossover distribution $Q(s;\omega,\eta)$ with appropriate values of (ω,η) is shown by broken lines. (b) Δ_3 statistics of Dyson and Mehta. Those of GOE and Poisson are shown by broken lines.
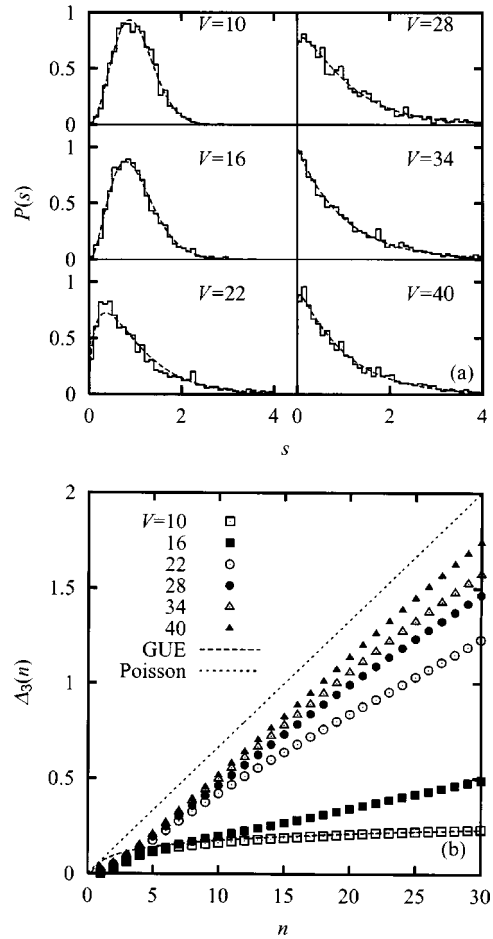

FIG. 3. The spectral statistics of a homogeneous phase with random magnetic fields $\xi = 0.1$ when V is taken to be 10, 16, 22, 28, 34, and 40. (a) The nearest-neighbor spacing distribution $P(s)$. The crossover distribution $Q(s;\omega,\eta)$ with appropriate values of (ω,η) is shown by broken lines. (b) Δ_3 statistics of Dyson and Mehta. Those of GUE and Poisson are shown by broken lines.

of Anderson transition features a continuous change in the ratio of chaotic to integrable sections in a wave-number space.

B. Heterotic phase

Let us turn to the case when $V_s \neq V_l$, which will be referred to as a heterotic phase. $V_s = 10$ and $V_l = 40$ are used in our numerical investigations. Note that when $M = 0$, the whole system is influenced by the degree of random potentials with V_l. When $M = L$, the degree of disorder is V_s over the whole structure, so our system is homogenous again. Because V_l is large enough to localize a quantum particle and V_s is small enough to let a quantum particle be diffuse, as M increases there is a transition from localized states to extended states.

Figure 4 shows the nearest-neighbor spacing distribution $P(s)$ and the Δ_3 statistics of Dyson and Mehta when M is changed from 2 to $L = 22$ with $\xi = 0$. If $M = 0$, the spectral statistics would be those when $V = 40$ in Fig. 2. On the other hand, if $M = L$, the spectral statistics would be those when

$V = 10$ in Fig. 2. Note that $P(s)$ of the observed spectra is well approximated by the broken lines, i.e., the crossover distribution $Q(s;\omega,\eta)$ with appropriate values of (ω,η). Figure 5 shows the nearest-neighbor spacing distribution $P(s)$ and the Δ_3 statistics of Dyson and Mehta when M is changed from 2 to $L = 22$ with $\xi = 0.1$. If $M = 0$, the spectral statistics would be those when $V = 40$ in Fig. 3. On the other hand, if $M = L$, the spectral statistics would be those when $V = 10$ in Fig. 3.

There is a transition region between $M = 0$ and $M = L$ where our structure has the properties of a superlattice [27]. In our structure, a quantum particle may be extended over the region with $1 \leqslant z_p \leqslant M$ because of the small degree of disorder. On the other hand, a quantum particle is apt to be localized near a site having low-potential energy in the region where $M + 1 \leqslant z_p \leqslant L$ because of the large degree of disorder. A quantum particle extended over the clean region is confined by the boundary between the two regions, as in a heterostructure of compound semiconductors [28–46]. Therefore, quantum states whose classical counterpart is chaotic inside the clean region expand smoothly as M increases
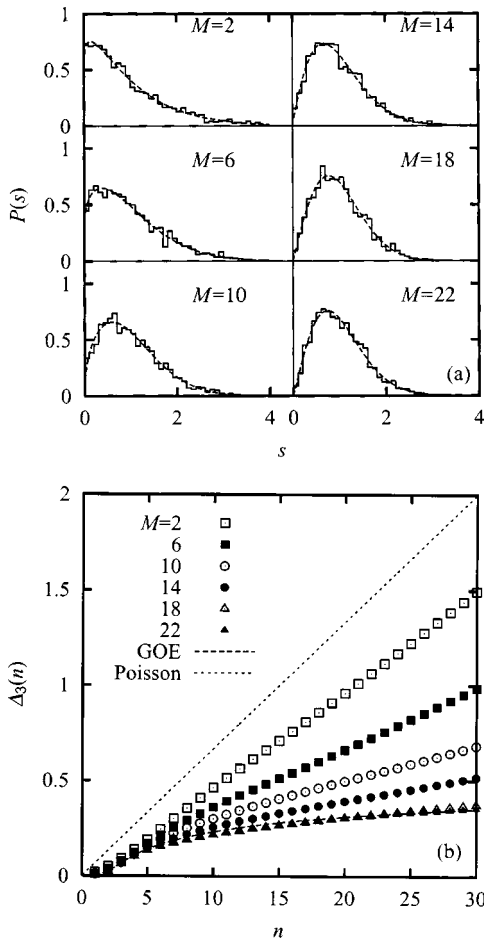
FIG. 4. The spectral statistics of a heterotic phase characterized by $V_s = 10$ and $V_l = 40$ without random magnetic fields $\xi = 0$ when M is taken to be 2, 6, 10, 14, 18, and 22. (a) The nearest-neighbor spacing distribution $P(s)$. The crossover distribution $Q(s;\omega,\eta)$ with appropriate values of (ω,η) is shown by broken lines. (b) Δ_3 statistics of Dyson and Mehta. Those of GOE and Poisson are shown by broken lines.

FIG. 5. The spectral statistics of a heterotic phase characterized by $V_s = 10$ and $V_l = 40$ with random magnetic fields $\xi = 0.1$ when M is taken to be 2, 6, 10, 14, 18, and 22. (a) The nearest-neighbor spacing distribution $P(s)$. The crossover distribution $Q(s;\omega,\eta)$ with appropriate values of (ω,η) is shown by broken lines. (b) Δ_3 statistics of Dyson and Mehta. Those of GUE and Poisson are shown by broken lines.

while the region of strong disorder, in which quantum states remain almost integrable, is reduced. This type of Anderson transition features a continuous change of the ratio of chaotic and integrable regions in real space.

C. Crossover characterization

Figure 6 shows the values of (ω,η) both for a homogenous phase and a heterotic phase characterized by $V_s = 10$ and $V_l = 40$. Random magnetic fields are introduced by $\xi = 0.1$ in Fig. 6(b), but $\xi = 0$ in Fig. 6(a). Let us look at the route in the (ω,η) plane when the heterotic phase is in a random magnetic field. When $M = 0$, we note that the system is essentially integrable, as indicated by $(\omega,\eta) = (0,0)$. When M increases and (ω,η) changes from $(0,0)$, η rapidly increases leaving ω unchanged. When $M = 4$, η reaches 1 with a very small value of $\omega = 0.1$. As M increases beyond 6, on the other hand, ω begins to increase. Note that the route of the heterotic phase from Poissonian to GUE goes along the upper side in the figure.
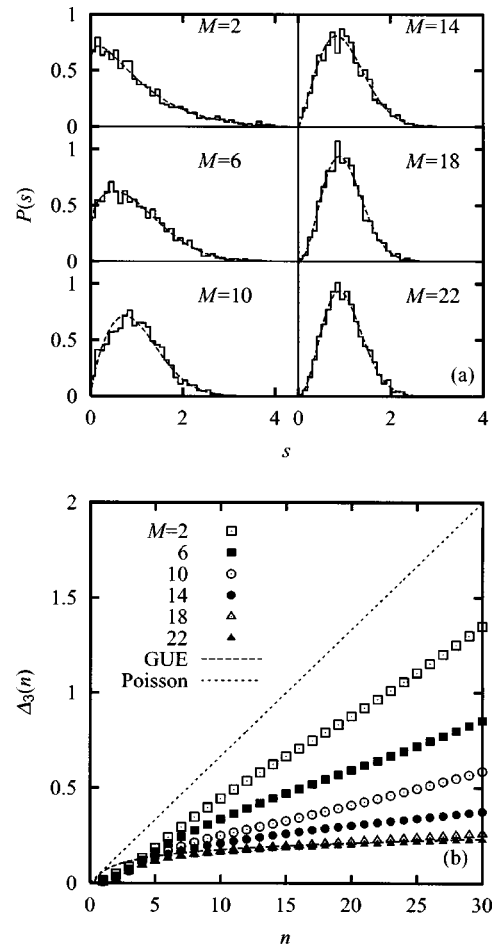
In a heterotic phase, a finite M creates a region which is characterized by quantum chaos. However, there remains a region of integrable systems, where degenerate levels exist, so ω is kept at a very low value. The energy levels of states whose classical counterpart has a chaotic orbit in the region where $z_p \lesssim M$ are sandwiched by adjacent energy levels of states whose classical counterpart is regular in the region where $M < z_p$, so relatively large intervals between adjacent levels are unlikely to appear in the spectrum of our structure, as suggested by the large value of η. This is a consequence of the coexistence of quantum chaotic and regular regions in real space.

Let us turn to the homogenous phase, in which $(\omega,\eta) = (0,0)$ corresponds to $V = 40$. The system remains integrable while V is decreased from 40 down to 28. As V is reduced below 28, (ω,η) changes from $(\omega,\eta) = (0,0)$. As it detaches from $(0,0)$, ω rapidly increases, leaving η small. Therefore, the route of the homogenous phase from Poissonian to GUE goes along the lower side of the figure, as opposed to that of the heterotic phase. This is a typical
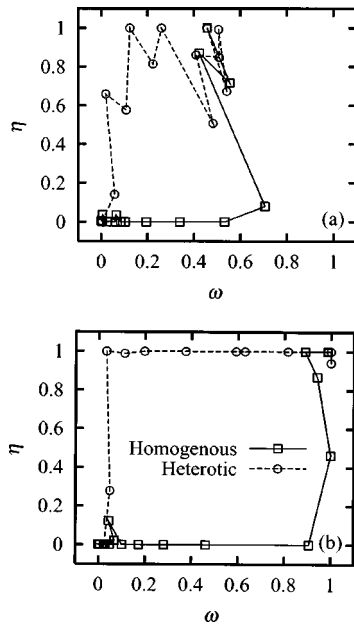
FIG. 6. Appropriate values of (ω, η) to characterize the nearest-neighbor spacing distribution (a) with no magnetic fields and (b) with random magnetic fields. The route from $(\omega, \eta) = (0,0)$ to $(1,1)$ along the upper side is attributed to a heterotic phase characterized by $V_s = 10$ and $V_l = 40$, where M takes $0, 2, 4, \ldots, 24$. The route along the lower side is attributed to a homogenous phase where $V_s = V_l = V$ takes $10, 12, 14, \ldots, 40$.

Anderson transition due to on-site random potentials in a cubic lattice, so a relatively large bandwidth encourages quantum particles to move over the whole structure in the quantum chaotic regime, resulting in a repulsion between energy levels. This is reflected in the remarkable change in ω. Routes in the (ω, η) plane are very different for these two types of structures and this difference is useful in distinguishing the transition from Poissonian to quantum chaos during a heterotic phase from that during a homogenous phase. The transition from Poissonian to GOE can be seen in Fig. 6(a), where there are no random magnetic fields, i.e., $\xi = 0$. The difference of routes in the (ω, η) plane can be understood in a similar way.

IV. DISCUSSION AND CONCLUSION

A true phase transition occurs only at the thermodynamic limit, where a quantum system occasionally decomposes into disjointed sectors between which there is no quantum coherence, although it is useful to consider an analog of phases in characterizing a finite system, in particular, nanosystems [47]. As the size of the system is reduced, the tunneling amplitude between sectors, which would be disjointed in the thermodynamic limit, rises, resulting in the onset of quantum coherence between the sectors. Because there is quantum coherence between a quantum system of finite particles which have the characteristics of phase A of an infinite system and a quantum system of finite particles which have the characteristics of phase B of an infinite system, our composite quantum system can be thought of as having the heterotic phase of phase A and phase B.

The type of the heterotic phase related to the density-driven Mott transition can be found in a quantum-dot array [48]. Let us consider a chain of quantum dots when the density of electrons is kept below that of half-filled electrons. The typical size of quantum dot is 10 nm if a compound semiconductor heterostructure is used to confine electrons in the dot. The field effect can cause a confining potential on the order of 100 nm, so a chain of quantum dots can be under a global confining potential with a parabolic shape [49,50]. As the global confining potential becomes stronger, the density of electrons around the center of the chain increases. When the density reaches that of half-filled electrons, these electrons in the center become insulating. On the other hand, electrons on the periphery remain metallic because their density is low. This is the heterotic phase of the Mott-insulating phase in the center and the metallic phase on the periphery [51].

A second type of heterotic phase, which is related to the bandwidth-driven Mott transition, is expected in a nerve-cell-like fractal-based complex [14]. There is a difference between the fractal dimension in the center of a nerve-cell-like complex, i.e., the somatic fractal, and that in the peripheral regions, i.e., the dendritic fractal [52]. It is possible to realize a heterotic phase of an Anderson insulator and a normal metal in our superlattice, as in a nerve-cell-like complex [53].

We have noted that the crossover characterization of the spectral statistics, specified by two parameters (ω, η), is useful in distinguishing the heterotic phase of an Anderson insulator and a normal metal in our structure from an intermediate phase of a disordered medium in which the degree of disorder is homogenous. During transitions from the Poissonian to the Gaussian unitary ensemble, the values of (ω, η) have a route from (0,0) to (1,1). The route during a heterotic phase of an Anderson insulator and a normal metal is very different from the route during a homogenous phase.

[1] S. W. McDonald and A. N. Kaufman, Phys. Rev. Lett. **42**, 1189 (1979).

[2] T. H. Seligman, J. J. M. Verbaarschot, and M. R. Zirnbauer, Phys. Rev. Lett. **53**, 215 (1984).

[3] O. Bohigas, M. J. Giannoni, and C. Schmit, Phys. Rev. Lett. **52**, 1 (1984).

[4] M. L. Mehta, *Random Matrices*, 2nd ed. (Academic Press, London, 1991).

[5] E. Heller, Phys. Rev. Lett. **53**, 1515 (1984).

[6] M. S. Hussein and M. P. Pato, Phys. Rev. Lett. **70**, 1089 (1993).

[7] E. Brézin, S. Hikami, and A. Zee, Phys. Rev. E **51**, 5442 (1995).

[8] E. Brézin, S. Hikami, and A. I. Larkin, Phys. Rev. B **60**, 3589 (1999).

[9] G. Lenz and F. Haake, Phys. Rev. Lett. **65**, 2325 (1990).

[10] A. G. Aronov, V. E. Kravtsov, and I. Lerner, Phys. Rev. Lett. **74**, 1174 (1995).

[11] M. V. Berry and M. Robnik, J. Phys. A **17**, 2413 (1984).

[12] B. Eckhardt, Phys. Rep. **163**, 205 (1988).

[13] T. A. Brody, J. Flores, J. B. Frenchy, P. A. Mello, A. Pandey, and S. S. M. Wong, Rev. Mod. Phys. **53**, 385 (1981).

[14] R. Ugajin, Appl. Phys. Lett. **80**, 4021 (2002); J. Appl. Phys. **92**, 5772 (2002).

[15] B. I. Shklovskii, B. Shapiro, B. R. Sears, P. Lambrianides, and H. B. Shore, Phys. Rev. B **47**, 11487 (1993).

[16] E. Hofstetter and M. Schreiber, Phys. Rev. B **49**, 14726 (1994).

[17] S. N. Evangelou, Phys. Rev. B **49**, 16805 (1994).

[18] I. Kh. Zharekeshev and B. Kramer, Phys. Rev. B **51**, 17239 (1995).

[19] E. B. Bogomolny, U. Gerland, and C. Schmit, Phys. Rev. E **59**, R1315 (1999).

[20] P. W. Anderson, Phys. Rev. **109**, 1492 (1958).

[21] E. Abrahams, P. W. Anderson, D. C. Licciardello, and T. V. Ramakrishnan, Phys. Rev. Lett. **42**, 673 (1979).

[22] P. A. Lee and T. V. Ramakrishnan, Rev. Mod. Phys. **57**, 287 (1985).

[23] E. Hofstetter and M. Schreiber, Phys. Rev. Lett. **73**, 3137 (1994).

[24] S. Hikami, A. I. Larkin, and Y. Nagaoka, Prog. Theor. Phys. **63**, 707 (1980).

[25] S. N. Evangelou, Phys. Rev. Lett. **75**, 2550 (1995).

[26] F. Haake, *Quantum Signatures of Chaos* (Springer-Verlag, Berlin, 1991).

[27] L. Esaki, IEEE J. Quantum Electron. **QE-22**, 1611 (1986).

[28] L. Esaki and L. L. Chang, Phys. Rev. Lett. **33**, 495 (1974).

[29] P. Manuel, G. A. Sai-Halasz, L. L. Chang, Chin-An Chang, and L. Esaki, Phys. Rev. Lett. **37**, 1701 (1976).

[30] A. S. Barker, Jr., J. L. Merz, and A. C. Gossard, Phys. Rev. B **17**, 3181 (1978).

[31] V. Narayanamurti, H. L. Störmer, M. A. Chin, A. C. Gossard, and W. Wiegmann, Phys. Rev. Lett. **43**, 2012 (1979).

[32] J. N. Schulman and T. C. McGill, Phys. Rev. B **19**, 6341 (1979).

[33] B. Jusserand, D. Paquet, and A. Regreny, Phys. Rev. B **30**, 6245 (1984).

[34] A. K. Sood, J. Menéndez, M. Cardona, and K. Ploog, Phys. Rev. Lett. **54**, 2111 (1985).

[35] C. Colvard, T. A. Gant, M. V. Klein, R. Merlin, R. Fischer, H. Morkoc, and A. C. Gossard, Phys. Rev. B **31**, 2080 (1985).

[36] A. Ishibashi, M. Itabashi, Y. Mori, K. Kaneko, S. Kawado, and N. Watanabe, Phys. Rev. B **33**, 2887 (1986).

[37] J. Bleuse, G. Bastard, and P. Voisin, Phys. Rev. Lett. **60**, 220 (1988).

[38] E. E. Mendez, F. Agulló-Rueda, and J. H. Hong, Phys. Rev. Lett. **60**, 2426 (1988).

[39] P. Voisin, J. Bleuse, C. Bouche, S. Gaillard, C. Alibert, and A. Regreny, Phys. Rev. Lett. **61**, 1639 (1988).

[40] A. H. MacDonald and H. C. A. Oji, Phys. Rev. B **38**, 8249 (1988).

[41] T. Ando, S. Wakahara, and H. Akera, Phys. Rev. B **40**, 11609 (1989).

[42] T. Ando and H. Akera, Phys. Rev. B **40**, 11619 (1989).

[43] X. L. Lei, N. J. M. Horing, and H. L. Cui, Phys. Rev. Lett. **66**, 3277 (1991).

[44] M. Holthaus, Phys. Rev. Lett. **69**, 351 (1992).

[45] C. Waschke, H. G. Roskos, R. Schwedler, K. Leo, H. Kurz, and K. Köhler, Phys. Rev. Lett. **70**, 3319 (1993).

[46] T. Ando, Phys. Rev. B **47**, 9621 (1993).

[47] *Handbook of Nanostructured Materials and Nanotechnology*, edited by H. S. Nalwa (Academic Press, New York, 2000), Vols. 1–5.

[48] R. Ugajin, Int. J. Mod. Phys. B **13**, 2689 (1999).

[49] R. Ugajin, Physica B **229**, 146 (1997).

[50] R. Ugajin, Physica B **240**, 128 (1997).

[51] R. Ugajin, Phys. Rev. Lett. **80**, 572 (1998); Phys. Rev. B **59**, 4952 (1999).

[52] R. Ugajin, Phys. Lett. A **277**, 267 (2000); Physica A **301**, 1 (2001).

[53] R. Ugajin, Int. J. Mod. Phys. B (to be published).